



## Trapping of laser-vaporized silver clusters in rare-gas matrices: Magnetic circular dichroism (MCD) studies of silver clusters in neon and argon matrix

J. T. ZOUEU\*, E. FARHI<sup>#</sup> and J.C. RIVOAL

*Laboratoire de Spectroscopie en lumière Polarisée,  
UPR A0005 CNRS et Université P. et M. Curie  
ESPCI, 10 rue Vauquelin, 75231 Paris Cedex 05, France*

### Abstract

Silver clusters have been prepared by laser-ablation metal clusters source, embedded in rare-gas matrices at helium temperature (below 5 Kelvin) and studied by magneto-optical spectroscopy. We designed and constructed this source to produce and trap metallic clusters (M) in rare-gas (RG) matrices at low temperature. Optimizing the condensation parameters (source geometry, M-RG ratio, pulses intensities, temperature and delay), we perform sufficient amount of particles for optical signal detection in rare-gas matrix at low temperature as our results show. The magneto-optical spectra of the obtained mixture show several distinct bands within the range 2.48 - 4.47 eV. Silver atom peaks can be clearly identified; allowing the remaining bands to be assigned to larger silver clusters sizes.

### Introduction

The field of clusters offers the opportunity to understand the evolution of the structures and properties of these intermediate systems between small molecules and bulk solids. The production of clusters with all types of materials has been until a recent date a challenge. Using the laser vaporization technique has then provided several advantages: In this case, the clusters production can be of all sizes, neutral or ionic, from metallic types to refractory materials or not. So far, standard laser vaporization source of clusters [1-3] has been used for gaseous phase or clusters supported studies. Recently, Kari Vaskonen et al [4] used the laser-vaporization technique to produce and trap alkali atom in rare gas matrices and made evidence for tight trapping sites in Ar, Kr and Xe matrices for Li and Na not observed for atoms generated by conventional Knudsen oven techniques. More recently, A. L. Stepanov [5] and al constructed a new laser-based evaporation/ablation source of high cluster yield and deposited yttrium clusters on quartz or carbon-coated transmission electron microscopy (TEM) grids at room temperature. In our experiment, the metallic clusters were produced by laser-vaporization technique and embedded in the rare gas also used by the source to cool the metal vapor.

On the other hand, W. Harbich et al [6-8] had produced by sputtering techniques a series of mass selected silver clusters ( $\text{Ag}_n$ ,  $n=3-39$ ) trapped in Argon, Krypton and Xenon matrices, in order to make an unambiguous assignment and the study of the optical absorption, excitation and fluorescence spectra of these clusters. Our experiment offers the opportunity to complete these results by magneto-optical (MCD)

---

*Present Address: (\*) Institut National Polytechnique, Département Génie Electrique et Electronique, B.P. 1083 Yamoussoukro (République de Côte d'Ivoire). (#) Groupe DS/CS, ILLA/156, ILL, Grenoble, France*  
@ a GNPHE publication 2005, [ajmp@fsr.ac.ma](mailto:ajmp@fsr.ac.ma)

measurements.

The optical signal detection in solid rare gas matrices requires supplementary restriction for laser vaporization source. The signal detection necessitates  $10^{11}$  particules/cm<sup>2</sup> and a typical dilution factor of the particles in the gas matrices rare of one to  $10^4$ . The deposition temperature must be almost constant. The rare gas used by the source to cool the plasma of the metal is the same as the one we used to form the host matrices.

In this article we present the description and optimization of the laser-vaporization clusters source we designed and constructed for low temperature metallic clusters spectroscopy. We studied samples of silver clusters produced by this source, embedded in neon and argon matrix and analyzed by excitation, absorption and magnetic circular dichroism (DCM) spectroscopy as function of the magnetic field and temperature.

### Devices:

The silver clusters are produced by the laser-vaporization source of the figure-1: A Nd<sup>3+</sup> / YAG laser with frequency-doubling pulse at 532nm provides the energy of ablation (Brillant, Quantel Corp., frequency repetition: 10 Hz; pulse duration: 4 ns; energy per pulse: 300 mJ). The laser is focused on a silver rod target (axis perpendicular to the light beam), which is rotated after each pulse so that fresh areas of the surface of the rod continue to be exposed to the laser. The rare gas (neon or argon) is injected through a pulsed valve into the source in a counter-propagating direction with the metallic plasma emission produced by the laser impact in order to cool the metal vapor. Both rare gas (RG) and silver particles (M) exit the source and are trapped either on a quartz microbalance for the metal density determination or on the cryostat sample support at liquid helium temperature for spectroscopic measurements.

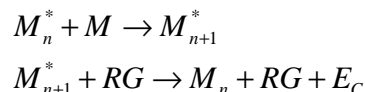
The Figure-2 gives the schematic of the spectroscopic measurements device already described in [9]. Absorption and MCD spectra are taken simultaneously. Radiation from a xenon arc lamp is passed through a monochromator, linearly polarized and modulated, split by a chopper with a rotating mirror (period T) and focused onto the sample. After traveling through the sample, the optical beam is split by, and synchronized with, a second chopper identical to the first. The reference and measurement beams are directed to the first photomultiplier (abs-PM). After traveling through the sample, the beam is collected by the second PM tube (dic-PM) between T/2 and T. Signals coming from both PMs are then demultiplexed, filtered, and sent to the computer.

To record excitation spectra the radiation from the monochromator excites the sample, with the whole emission collected at right angles to the incoming light. Again, the first chopper modulates the incident beam. The emitted light, focused on a third PM (fl-PM), is demodulated using a lock-in amplifier. The same configuration is used to record the fluorescence spectra. The first monochromator is fixed at one wavelength and a second monochromator inserted between the emitted light and the fl-PM analyses the emitted fluorescence.

### Experiments and discussions:

#### A) Description of the laser vaporization source

The cluster formation process in the laser-vaporization source results from M-M and M-RG interaction:



$n$  is the size of the cluster, the \* indicates an excited state and  $E_C$  is the excess energy transferred to the RG.

In this experiment, we are interested in the small size distribution (<10) study.

The clusters size distribution intensity ( $I_n$ ) depends on the source conditions and can be expressed as a function of the most important parameters such as the metal-vapor density ( $\rho_M$ ), the collision cross section ( $\sigma_{M-M}$ ), the temperature of the metal vapor ( $T_M$ ), the delay between the RG pulse and the laser pulse ( $\Delta_{RG-M}$ ), the pressure of the carrier-gas atoms ( $P_{RG}$ ) and the pressure outside of the source ( $P_V$ ):

$$I_n = f(\delta_M, \sigma_{M-M}, T_M, \tau_{RG-M}, P_{RG}, P_V)$$

The high RG instantaneous pressures in the source and the adiabatic supersonic expansion outside the source, causing the cluster formation, achieve the cooling of the metal vapor.

In order to achieve a small clusters size range ( $n < 10$ ), we design and construct the source with the follow characteristics:

- Neon and argon are used as rare gas (RG); this to reduce the collision cross-section for small cluster;
- The source is designed with  $V_{in}=4,67\text{cm}^3$  and  $V_{out}=3000\text{cm}^3$ ;  $V_{in}$  being the volume inside the source and  $V_{out}$  the volume outside the source;
- The pressure of the RG in the pulsed valve is 5,5 bars and 120 mbars in the source;
- The maximum temperature of the ejected plasma is 5000K;
- The nozzle diameter is 4mm.

The pulse duration of the RG is  $60\mu\text{s}$  and the admitted RG in the source pressure and temperature is evaluated with [10]:

$$T = T_0 \left( 1 + \frac{\gamma-1}{2} M^2 \right)^{-1}$$

$$P = P_0 \left( 1 + \frac{\gamma-1}{2} M^2 \right)^{-\frac{1}{\gamma-1}}$$

$$M = A \cdot \left( \frac{x-x_0}{D} \right)^{\gamma-1} - \frac{1}{2A} \cdot \frac{\gamma+1}{\gamma-1} \left( \frac{x-x_0}{D} \right)^{\gamma-1}$$

Where  $M$  is the Mach number,  $A$  is nozzle area, and  $P_0, T_0$  and  $x_0$  the initial conditions.

The density and the temperature of the metal vapor produced by the laser-vaporization is evaluated by the equation proposed by A. T. Prengel and al [11]:

$$n(t) = \frac{d\pi r^2}{k} \left( \frac{m}{2\pi k} \right)^{\frac{3}{2}} \int_0^t \frac{p[T(t')]}{[T(t')]^{\frac{5}{2}} [t-t']^4} \exp\left(-\frac{md^2}{2kT(t')(t-t')^2}\right) dt'$$

Here  $d$  is the distance from the heated surface to the resonance beam light used to measure the absorption proportional to the density,  $k$  the Boltzmann constant,  $m$  is the atomic mass and  $p[T]$  is the equilibrium vapor pressure corresponding to the time dependent surface temperature  $T$  of the rod, given by

$$T(t) = T_a + (T_0 - T_a) \left[ 1 - \exp\left(-\frac{r}{4\kappa t}\right) \cdot \text{erf} \left[ \frac{\epsilon}{(4\kappa t)^{\frac{1}{2}}} \right] \right]$$

$T_a$  is the ambient temperature of the surrounding medium,  $T_0$  the temperature of the rod of length  $2l$  and  $\kappa$  is the thermal diffusivity in  $\text{cm}^2/\text{sec}$ .

The optimal theoretical laser intensity for the pulsed laser calculated is  $I_S = 9,35 \cdot 10^{11}$  Watts/ $\text{cm}^2$ . In practice  $I = 1,44 \cdot 10^9$ W/ $\text{cm}^2$  was necessary; this can be explained by the bad rod surface quality and the absorber impurities in the metal. The calculated RG velocity at the outside of the pulsed valve is 1700m/s ( $M=5,3$ ) and the velocity of the ejected metal is approximated to 1km/s. The vaporization begins one picosecond's after the absorption of the entire laser energy and the vaporization takes ten picoseconds. The time necessary to the RG to attain the metal rod is  $85\mu\text{s}$ . In order to achieve the optimal condition of the metal vapor supersaturating, the laser pulse must operate  $100\mu\text{s}$  after the pulsed valve opening. We have determined experimentally  $87\mu\text{s}$ .

In our experiments, we preferred a pulsed valve with short open duration (10Hz; 0-500 $\mu\text{s}$ ) as a substitute

of the general valve that produces a quasi-continuous flow of gas. The reason is that the rare gas used to cool the plasma ( $\approx 4500\text{K}$  calculated) is the same used to form the matrices, which must be transparent ( $M/RG \approx 10^{-4}$ ). We then achieved the best pumping condition in the vacuum chamber ( $10^{-6}\text{mbar}$ ). The typical running time duration of the clusters source is 10 mn per sample. This corresponds to  $\approx 100$  monolayers ( $1,4 \cdot 10^{15}$  metal atoms measured by quartz microbalance).

1) In order to avoid fragmentation of the cluster in the zone of silence, we determined experimentally 4mm for the diameter of the output source orifice and locate a skimmer at 5mm after the output of the source. The source volume is about  $4,67\text{cm}^3$  and the rare gas pressure inside the source is about 4bars. We located a fast ionization gauge at 10 cm from the output of the cluster source and measured a length of the pulse to be 44,8 cm. The fluorine sample support was situated at 26 cm from the clusters source.

2) We obtained a maximum quantity of metal at the output when the laser ablation operates at  $87\mu\text{s}$  after opening the pulsed valve that last  $200\mu\text{s}$ .

We measured  $1,47 \cdot 10^{12}$  atoms by pulse with the quartz microbalance placed at 5mm from the output of the source. The calculation of the metal inside the source has been done by measuring the dimension of the crack made by the laser ablation impact on the silver target with optical microscopy techniques; we obtained  $30\mu\text{m}$  for the diameter of the hole and  $200\mu\text{m}$  for its depth. This corresponds to ejected silver atoms of  $10^{17}$  by pulse. The laser intensity used was  $1,44\text{GW}/\text{cm}^2$ . The major parts of the metal stick themselves and covered the surface inside the clusters source because of the high temperature of the plasma.

3) For this experiment, we found out a satisfactory conical geometry nozzle of 4mm diameter for the experimental conditions above.

## B) Results and discussion

We realized two types of sample in the previous characterized experimental condition; the first sample consists of depositing silver particle in argon matrix and the second silver in neon matrices.

### 1) First experiment: silver in argon matrix

The figure-3 gives the: Absorption spectrum (a), DCM spectra as function of the applied magnetic field (b), DCM spectra as function of temperature (c), Excitation spectra as function of low pass filters (d) and (e) and Fluorescence spectra (f) and (g).

The above seven spectra reveal three well known separated optical transitions at  $31748\text{cm}^{-1}$ ,  $32864\text{cm}^{-1}$  and  $33505\text{cm}^{-1}$ , which correspond to the silver atom [12]. In this experiment the percentage of atoms is very large because of the temperature of the plasma inside the cluster source is high so that a weak part the atoms is cooled.

Apart of the atoms well-known bands [12], we observed a large band from  $29500\text{cm}^{-1}$  to  $31500\text{cm}^{-1}$  on the absorption spectrum (a). This broadened band is split in two bands on the MCD spectra and grows with the magnetic field (b) and when the temperature of the sample (c) decreases. This region corresponds to the transitions of the small silver clusters sizes. We observed a very large additional band from  $28000\text{cm}^{-1}$  to  $35000\text{cm}^{-1}$  that varies with the magnetic field.

In excitation spectrum the incident light on the sample varies between  $28000$  and  $35000\text{cm}^{-1}$  and we record the total fluorescence remaining at an energy below filter's cut-off. The spectra (d) with the low pass filter at  $22220\text{cm}^{-1}$  show two significant optical bands at  $30000\text{cm}^{-1}$  and  $30600\text{cm}^{-1}$ , in addition to the atomic bands. The amplitude of these bands is comparable to the atomic one with this filter but clearly decreases when the cut-off frequency of the filter increases (see fig 3(e)). Relatively to the absorption and DCM amplitudes of the atomic transitions, we can observe that these species fluoresce more than the atoms in a restricted energy range. To clarify that point we recorded the fluorescence spectra while exciting the sample at fixed wavelengths namely  $30000$  and  $30620\text{cm}^{-1}$  corresponding at these new bands. As shown in fig 3 (f) the fluorescence spectra is markedly different from the one of the atom taken while exciting in the atomic bands (see fig 3 (g)). It is clear that these bands can't be a second atomic site bands. The clusters which transitions energies are closer to that are  $\text{Ag}_3$  ( $29561\text{cm}^{-1}$ ),  $\text{Ag}_5$  ( $29560\text{cm}^{-1}$ ),  $\text{Ag}_7$  ( $30689\text{cm}^{-1}$ )  $\text{Ag}_9$  ( $30318\text{cm}^{-1}$ ) and  $\text{Ag}_{11}$  ( $30497\text{cm}^{-1}$ ). Comparing the fluorescence spectrum of the exciting band at  $30620\text{cm}^{-1}$  to those obtained by W. Harbich et al, we can assign this band to  $\text{Ag}_7$ .  $\text{Ag}_n$  (n

= 2-11) are also expected in this region. The excitation spectrum with the low pass filter at  $21053 \text{ cm}^{-1}$  fig 3 (d) shows another band at  $34400 \text{ cm}^{-1}$ . This band, which is probably superposed with other band according to its large width presents a positive DCM signal. Comparing to the data of W. Harbich et al, this band can be assigned to  $\text{Ag}_{11}$ .

The large broadened band observed from 28000 to 35000 can be explained by the presence of the others transitions of the observed clusters ( $\text{Ag}_n$ ,  $n=2-11$ ). This is confirmed by the fact that the peak-to-peak evolution of the atomic transition as function of the magnetic field in non-linear.

A mass selected analysis must complete these results.

## 2) Second experiment: silver in neon matrix

The figure-4 gives magneto-optical spectra of the sample realized with silver target and neon as rare gas: (a) Absorption spectrum and (b) DCM spectra as function of the applied magnetic field.

The two spectra 4(a) and 4(b) exhibit several distinct bands; the well known atomic bands (range  $30000-34000 \text{ cm}^{-1}$ ) corresponding to the  $P \leftarrow S$  resonance are clearly identified; the remaining peaks are then assigned to clusters which sizes are larger than mono-atomic silver.

We observed (absorption and DCM spectra) in the range  $20000 - 30000 \text{ cm}^{-1}$  that there are at least three large bands and two peaks at  $34000 \text{ cm}^{-1}$  and  $35300 \text{ cm}^{-1}$ . The bandwidths average length of the cited peaks in this range is about  $4000 \text{ cm}^{-1}$ . The two major bands observed in this region correspond to a superposition of several peaks, which, we attribute to dimeric and trimeric silver. In the argon matrix, we have detected the sizes bigger than seven. So, we expected to have smaller sizes in neon matrix because of the lower M/RG cross section. Fedrigo and Harbich had reported in previous work, dimers and trimers optical spectra in argon matrix. They identified three bands centered at ( $26180, 38170, \text{ and } 42740 \text{ cm}^{-1}$ ) which were attributed to dimers and three other bands centered at ( $31150, 25910, 20330 \text{ cm}^{-1}$ ). It had been also observed an average blue shift of  $800 \text{ cm}^{-1}$  of silver clusters in rare gas matrices going to xenon to neon; so we expected to detect some optical bands which can be assigned to dimers and trimers in the range  $20000 - 30000 \text{ cm}^{-1}$ . These optical bands exhibit DCM signals. On the other hands, the bigger sizes like  $\text{Ag}_5$  or  $\text{Ag}_7$  present optical lines in the range of atomic transitions. The variation of the relatives observed peaks in this region from the absorption to DCM spectra could be explained by the presence of other peak about the atoms. To confirm this assumption, we studied the relatives' peaks variation as function of the temperature and the magnetic field; this is non-linear. Furthermore, these lines never show the same relative intensity evolution under additional M/RG deposition. It can therefore be concluded that these bands correspond to several species including silver atom. These supplementary sizes are expected to be  $\text{Ag}_5$  and  $\text{Ag}_7$ .

These optical and magneto-optical studies of the silver particles in argon and neon matrices demonstrate that we form silver clusters with small sizes and these small sizes exhibit a DCM signal.

## 3) summarizing

In these matrices (neon and argon), we have deposited a small silver cluster's statistical mass distribution. In respect to the important quantity of atoms detected in the matrices, the typical sizes expected are about ten atoms; this is due to the high temperature of the metal vapor. The theoretical calculation based on the spherical jellium model for metal clusters and experimental data have shown that the stable sizes detected are  $N=8, 18, 20, 34, 40, 58, 92\dots$ . So the principal observed bands should be assigned to  $\text{Ag}_8$ . The observed transitions attributed to  $\text{Ag}_7$  can be explained by fragmentation ( $\text{Ag}_8 \rightarrow \text{Ag}_7 + \text{Ag}$ ) operating between the source and the sample support.

When the studied species are paramagnetic, they exhibit DCM spectra under magnetic field perturbations; in the case of silver cluster, the DCM signal are expected for the sizes of  $\text{Ag}_{(2n+1)}$ ; This confirms the DCM signal detected for  $\text{Ag}_7$ . Under the magnetic field, the DCM magnitudes are proportional to  $\frac{g\mu_B B}{W}$ , where

$W$  corresponds to the gap of electronic energies states. The spectra (b), (c) and (g) showed that DCM signal of the small silver particles distribution ( $n=2-11$ ) embedded in neon and argon matrices increased with  $B/T$  and prove that the Zeeman splitting effect is operative for the small silver clusters ( $n=11$ ).

This opens new perspectives towards the magneto-optical studies of metal clusters, coupling laser-ablation

clusters sources with mass selected apparatus.

### Conclusion:

We have built and optimized a cluster source, based on laser vaporization, which has been used to form a distribution of silver clusters embedded in argon and neon matrices. Using the absorption spectra of silver clusters produced by sputtering source and masse selected reported by Fedrigo and Harbich, we demonstrate that we formed small silver size cluster in argon and neon matrices like  $Ag_n$ ,  $n=2-11$ . We showed that these clusters could have a non-zero DCM signal indicating a degenerate ground state.

### REFERENCES:

- [1] V. Dupuis, J. P. Perez, J. Tuaille, P. Melinon, and A. Perez, J. Appl. Phys. 76 (10), 15 November 1994
- [2] Shigeo Maruyama, Lila R. Anderson, and Richard E. Smalley, Rev. Sci. Instrum. 61 (12), December 1990
- [3] V. E. Bondibey, Science, Vol 227, N° 4683 11January 1985
- [4] Kari Vaskonen, Jussi Eloranta, Henrik Kunttu, Chem. Phys. Let. Vol. 310 (1999) 245-251
- [5] A.L. Stepanov, M. Gartz, G. Bour, A. Reinhold, U. Kreibig, Vacuum 67 (2002) 223-227
- [6] W. Harbich, S. Fedrigo and J. Buttet, Chem. Phys. Let. Vol.195, n° 5,6 (1992) 613-617
- [7] S. Fedrigo, W. Harbich, J. Belyaev and J. Buttet, Chem. Phys. Let. Vol.211, n°2, 3 (1993) 166-169
- [8] C. Félix, C. Sieber, W. Harbich, and J. Buttet, Phys. Rev. Let. Vol.86, n°14 (2001) 2992-2995
- [9] J.T. ZOUEU, M. VALA and J.C. RIVOAL, Chemical Physics, 2004, (Available on line at [www.sciencedirect.com](http://www.sciencedirect.com) )
- [10] Landau, Lifchitz, "Mécanique des fluides" éd. Mir (Moscou) (1971)
- [11] A. T. Prengel, J. Dehaven, E. J. Johnson, and P. Davidovits, J. of Applied Physics, Vol. 48, N° 8, (1977) 3551-3556.
- [12] W. SCHULZE, H. U. BECKER and D. LEUTLOF, J. Phys. (Paris), 38 C2 (1977) 7

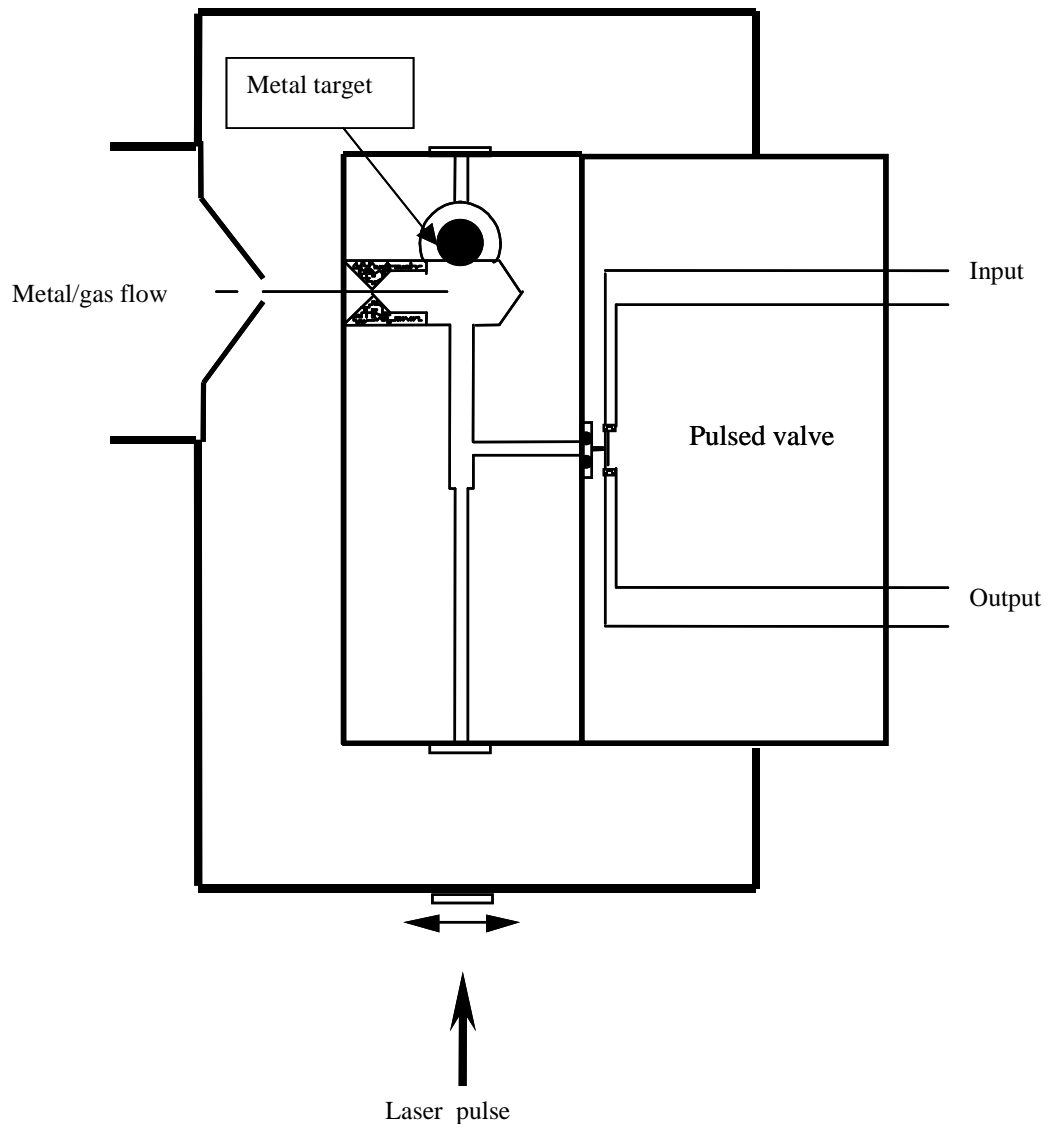


Figure-1 : Cluster source

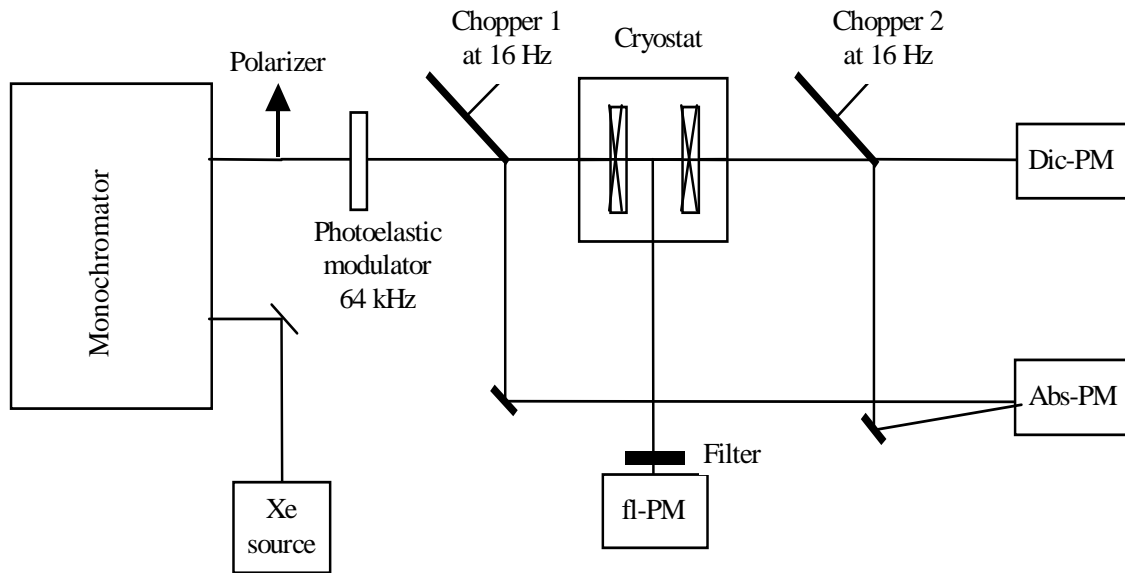
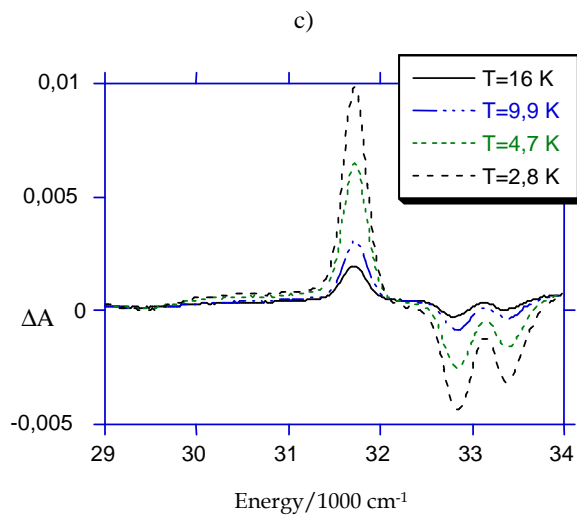
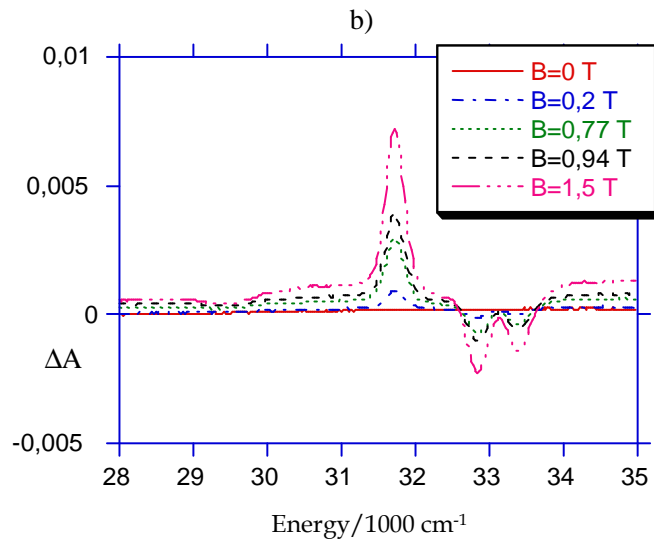
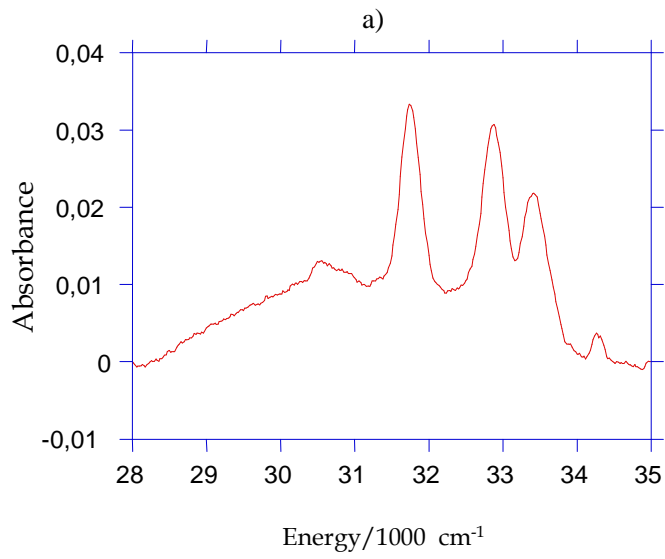
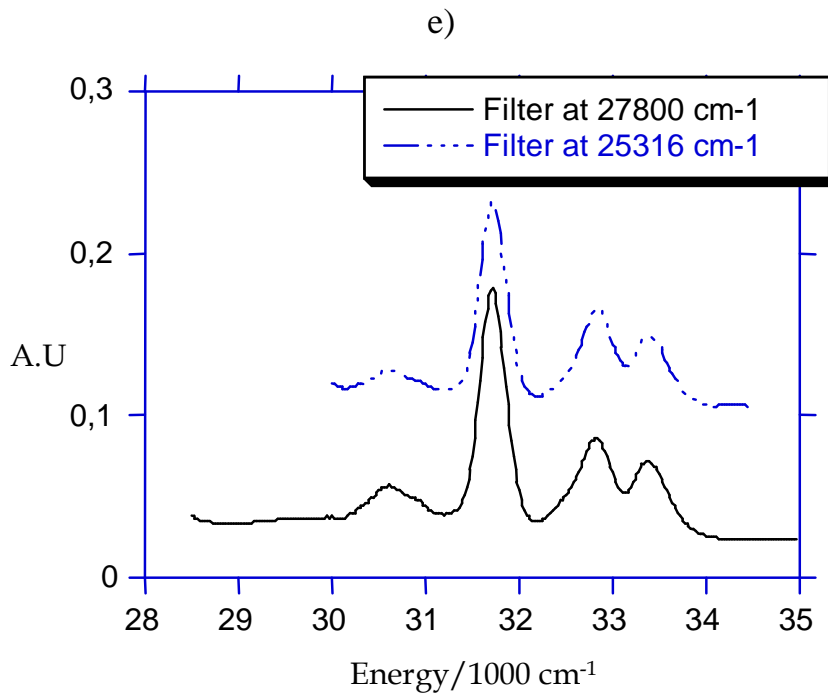
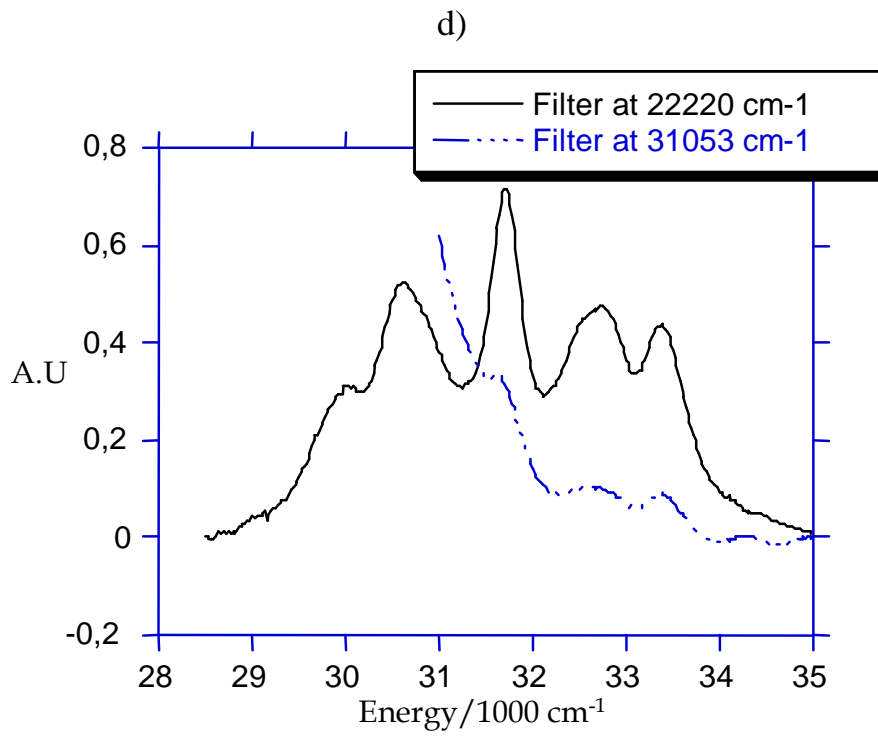


Figure-2 : Optical device





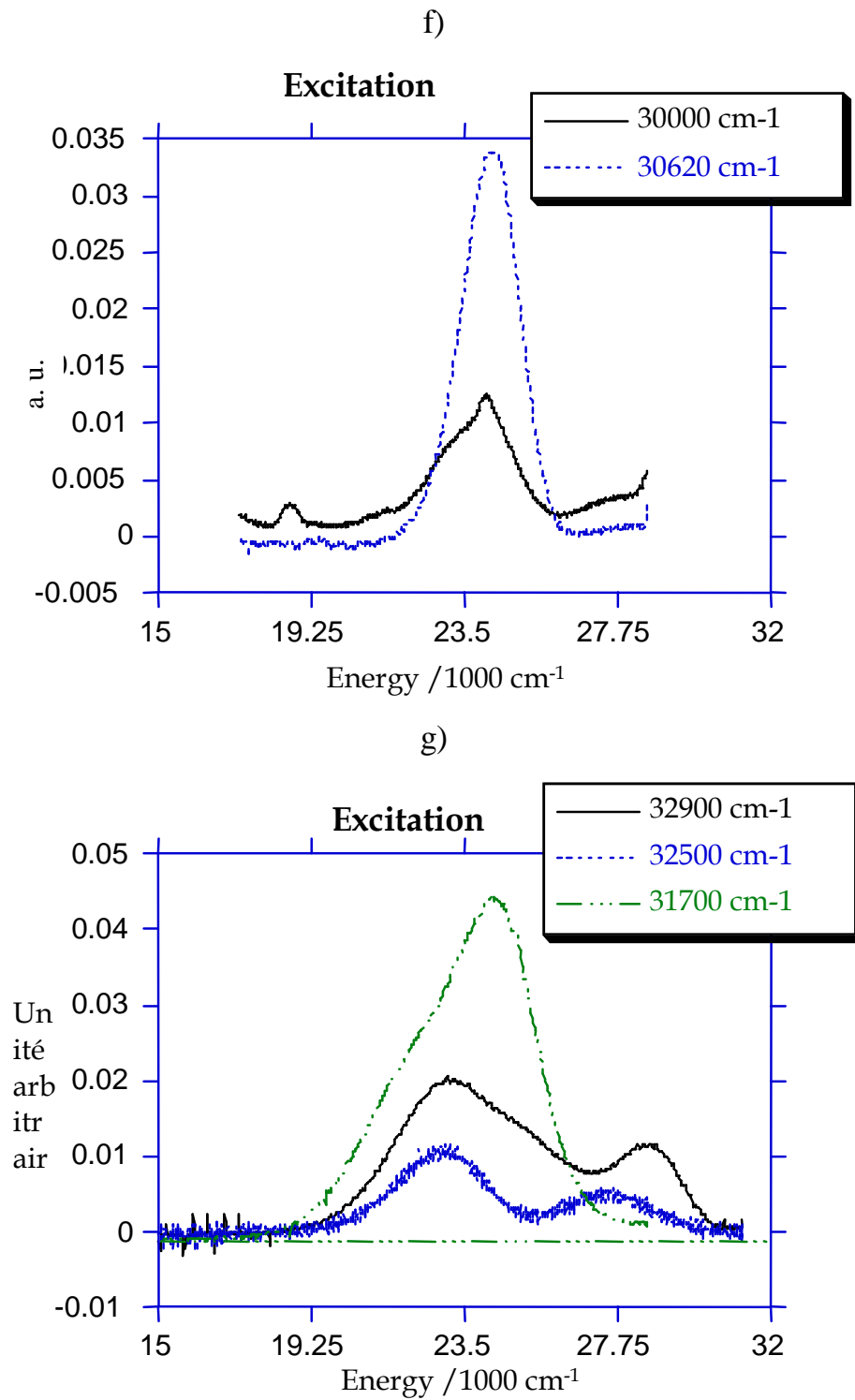


Figure-3 : Silver in argon matrix

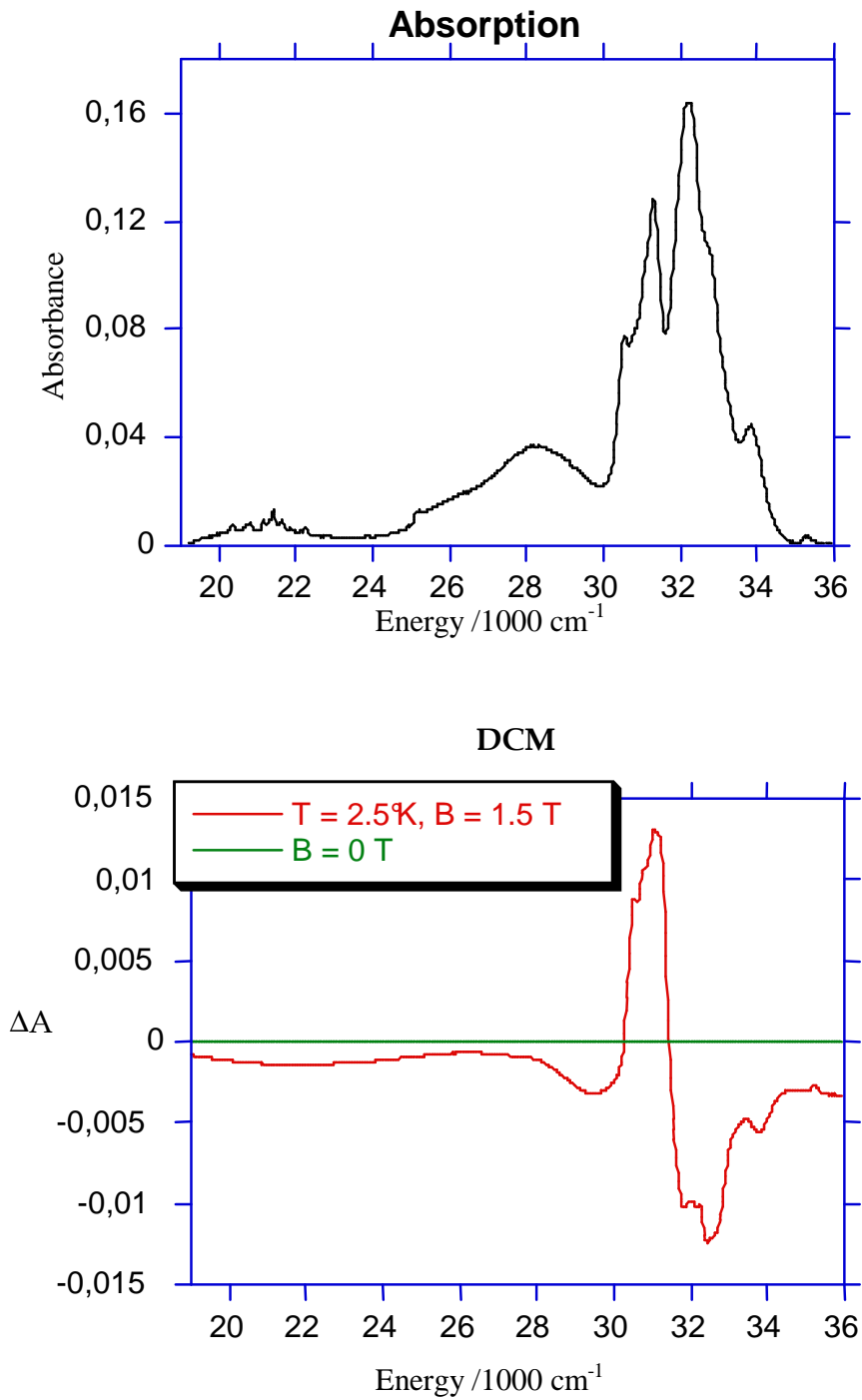


Figure-4 : Silver particles in neon matrix